4-4 Effect of Unit-cell Arrangement on Performance of Multi-stage-planar Cavity-free Unileg Thermoelectric Generator Using Silicon Nanowires

Katsuki Abe
Waseda University
Tokyo, Japan
katsube.aki@akane.waseda.jp

Kaito Oda
Waseda University
Tokyo, Japan
oda-fringe@moegi.waseda.jp

Motohiro Tomita
Waseda University
Tokyo, Japan
m.tomita3@aoni.waseda.jp

Takeo Matsuki
Waseda University, AIST
Ibaragi, Japan
takeo-matsuki@aist.go.jp

Takashi Matsukawa
AIST
Ibaragi, Japan
t-matsu@aist.jp

Takanobu Watanabe
Waseda University
Tokyo, Japan
watanabe-t@waseda.jp

***Abstract*— We compare the thermoelectric (TE) performances between two types of unit cell arrangements of planar unileg TE generators of silicon-nanowire (Si-NW). The planar TE generators are driven by the temperature gradient along the Si-NW. The TE performance highly depends on how the hot and cold sides of the unit cell is oriented with respect to the neighboring cells. If the hot sides of neighboring cells are placed next to each other, TE power is improved compared to the case where the hot and cold side of TE generator is arranged alternately. Optimal conditions of Si-NW length and metal wiring structure are also discussed.**

Keywords—Thermoelectric generator, Si, Nanowire, Semiconductor

I. Introduction

Energy harvesting such as TE power generation is expected as a new power source technology for the autonomous IoT system. Recently, it has been revealed that nano-sized Si shows excellent TE conversion ability [1]. Our research group proposed a cavity-free planar TE generator using Si-NW [2]. Generally, the output power of single TE generator is small to drive a DC/DC boost converter [3]. Thus, a large number integration of the TE generator is required to develop the output power.

We have investigated two types of unit cell arrangements to achieve the optimum structure which maximizes the power generation of the large-scale integrated cavity-free planar TE generators by means of FEM simulation. TE generators are categorized into two groups: unileg and bileg TE generator. An unileg TE generator is composed of only n-type or p-type semiconductor, and a bileg TE generator is composed of both n- and p-type types semiconductors. Bileg generators are advantageous to achieve high conversion efficiency between heat and electricity, but the unileg TE generators are also beneficial to reduce the manufacturing cost, and hence, to reduce the cost per power generation from ambient heat energy [4].

In cavity-free planar TE generators, the key to an efficient operation is how the temperature difference across the Si-NW is maintained. To do so, it is important to control the heat flow into the TE generator. In our previous studies [5,6,7], we reported the effects of the substrate structure and electrode area on the TE performance. In the present work, we focus on how to arrange the element of the unileg TE generator into an integrated TE module.

One of the arrangement of unileg TE generator is H-C-H-C arrangement where the hot and cold side of TE generator is arranged alternately as Hot-Cold-Hot-Cold…. However, the distance between the hot and cold side of neighboring TE generators is close to each other. As the result, the temperature difference will be diminished due to the heat leakage from the hot side to the cold side.

We propose C-H-H-C arrangement where the hot side of TE generator is arranged next to each other [7]. This arrangement is realized by a meander wiring [8]. In this study, we compare the TE performance of H-C-H-C and C-H-H-C arrangement of the cavity-free planar TE generators by FEM simulation.

II. Simulation Method

The model used in FEM calculation are shown in Fig. 1 and 2. Figure 1 and 2 show a cross-sectional view of the unit cell and the bird's-eye view of the 1st Al wiring layer and underlying layer of the unileg TE generator with H-C-H-C and C-H-H-C type arrangement, respectively. Figure 3 shows the top views. C-H-H-C arrangement requires a meander electric wiring to connect the hot and the cold side electrodes. To minimize the circuit footprint, the Al-bridge connecting hot and cold side is passed over the TE generators, but the structure has a slight drawback that the heat flow from the heat guide toward TE generator is impeded at the Al bridge, which will be discussed later.

COMSOL Multiphysics® 5.3 was used for the FEM simulation. The thermal and electrical conductivities of Si-pads, Si-NWs and SiO_2 layer are summarized in Table I. The employed equations in the simulation are summarized in Table II.

Table I Thermal conductivities and electrical conductivities used in FEM simulation

	Si-pad	Si-NW	SiO_2
Thermal conductivity [W/m·K]	131	1.4	1.4
Electrical conductivity [S/m]	232	232	

Table II The equations employed in this study

	Formula	
Heat transfer equation	$\nabla\ (\boldsymbol{q}+\boldsymbol{q_e})=0$	(1)
Fourier's law	$\boldsymbol{q}=k\ \ \nabla T$	(2)
Second Thomson relation	$P=ST$	(3)
Seebeck equation	$\boldsymbol{J_e}=-\sigma S\nabla T$	(4)
Peltier equation	$\boldsymbol{q_e}=P\boldsymbol{J}$	(5)
Current continuity equation	$\nabla\ \ \boldsymbol{J}=Q_{j,v}$	(6)
Ohrm's law	$\boldsymbol{J}=\sigma(-\nabla V)+\boldsymbol{J_e}$	(7)

In Table II, $\boldsymbol{q}$ is the heat flux caused by the temperature gradient, $\boldsymbol{q_e}$ is the Peltier heat flux, T is the temperature, k is the thermal conductivity, P is the Peltier coefficient, S is the Seebeck coefficient, $\boldsymbol{J_e}$ is the TE current, σ is the electrical conductivity, $\boldsymbol{J}$ is the total current density, $Q_{j,v}$ is the change of charge density per unit of time and V is the electric potential. The heat current distribution was simulated by simultaneously solving (1) - (5). The electric current was obtained by solving (3) - (7). The above calculations are repeated until both heat current distribution and electric current reach a steady state. A two-dimensional periodic boundary condition is adopted in x and y-axis (Fig. 1(b) and 2(b)).

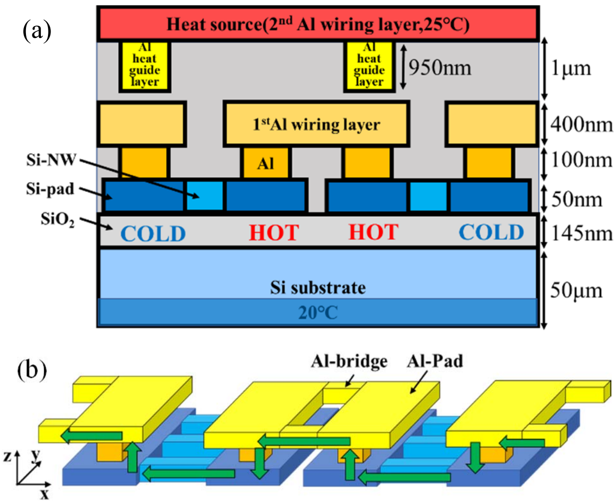

Fig. 1 Schematic of H-C-H-C device (a) cross section view, (b) Bird's-eye view. The green arrows show the current through the device.

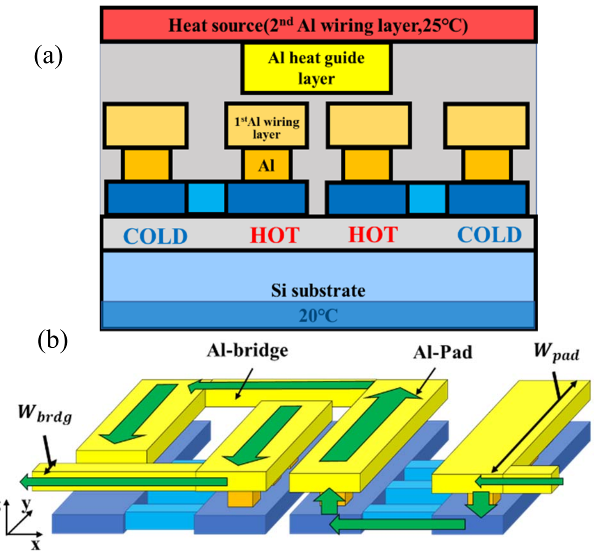

Fig. 2 Schematics of the unit cell of C-H-H-C device. (a) Cross-sectional view. (b) Bird's-eye view.

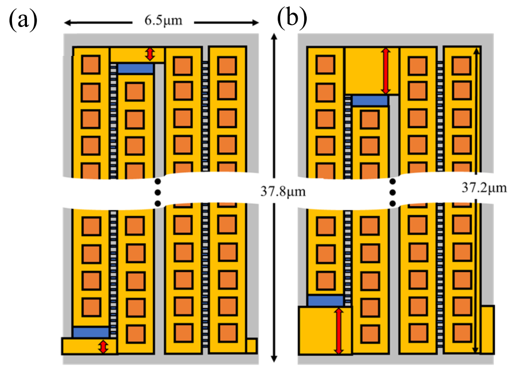

Fig. 3 Schematics of the unit cell of C-H-H-C device. Top view of the 1st Al wiring layer and underlying layers. Red arrow shows the W_{brdg}. (a) The $W_{brdg} \leq$. 1.8 μm. (b) The $W_{brdg} >$ 1.8 μm. In case of (b), the Al-pad width (W_{pad}) on the hot side becomes narrower than the W_{pad} when the W_{brdg} = 1.8 μm.

In this paper, the interconnecting Al-bridge width (W_{brdg}) of 1.8 µm and the Si-NW length (L_{NW}) of 250 nm are used as reference values. Then, the W_{brdg} was varied from 0.1 µm to 37.2 µm to find the optimum W_{brdg}. Furthermore, the L_{NW} was varied from 250 nm to 1000 nm to find the optimum L_{NW}. The TE power per unit area of the two types of unit cell arrangements were compared.

III. RESULTS&DISCUSSION

The highest TE power and power density of the C-H-H-C type were achieved to 1.61 nW and 655 µW/cm^2, respectively, when L_{NW} = 250 nm and W_{brdg} = 1.8 µm. The TE power and power density of H-C-H-C type were 1.13 nW and 459 µW/cm^2, respectively. Figure 4 and 5 show the cross-sectional temperature distributions. Figure 6 shows the temperature profile at the Si-NW surface along its longitudinal direction which is extracted from Fig. 4 and 5. Figure 6 shows the temperature profiles in the Si-NW for H-C-H-C and C-H-H-C type devices.

The temperature difference between both ends of Si-NW in C-H-H-C type is larger than that of H-C-H-C type. The temperature at the hot side of C-H-H-C type is maintained higher than that of H-C-H-C type due to decreasing the heat leakage from the hot side to the cold side. The injection pitch of the heat current has a greater impact on the TE performance, even if the wiring part partially impedes the heat current as shown in Fig. 7. The heat current leakage through the Al-bridge will have an unignorable impact on the performance of the TE generator if we shrink the device width in y-axis (see Fig.7(a)).

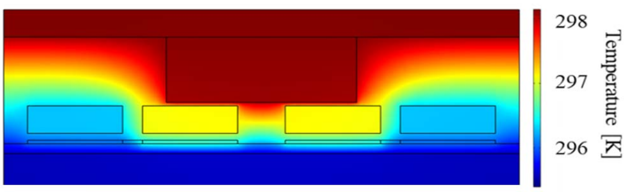

Fig. 4 Cross-sectional temperature distribution in C-H-H-C device (L_{NW}=250 nm, W_{brdg} = 1.8 µm)

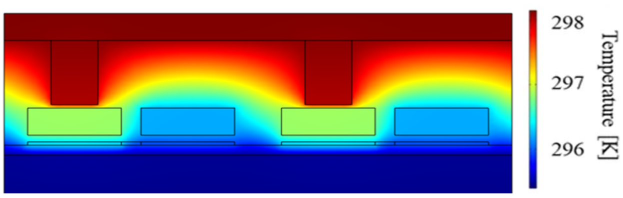

Fig. 5 Cross-sectional temperature distribution in H-C-H-C device (L_{NW} = 250 nm, W_{brdg} = 1.8 µm)

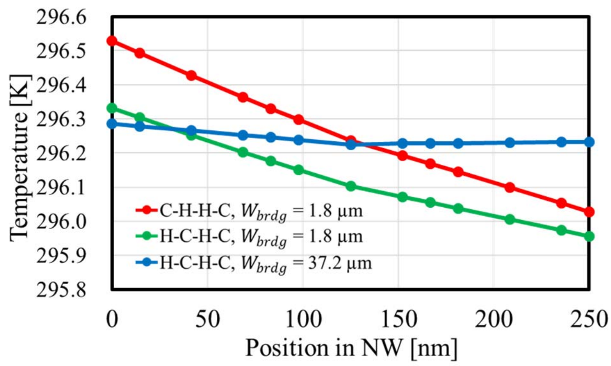

Fig. 6 One dimensional temperature profiles along the Si-NW

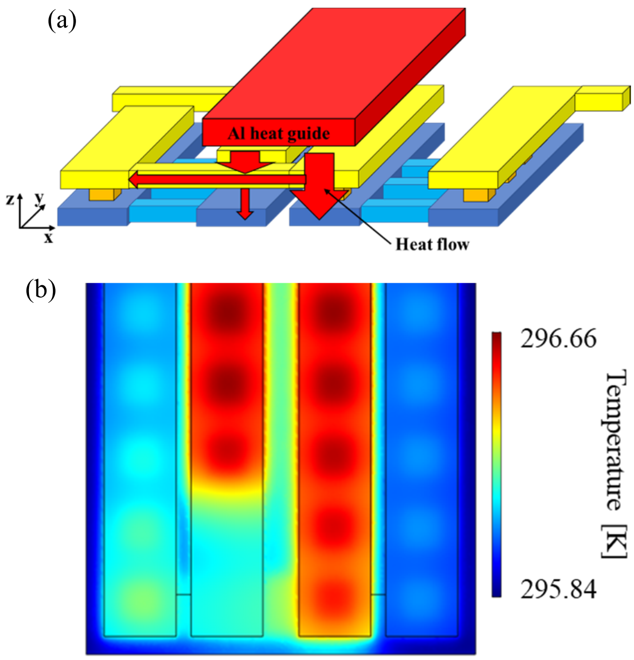

Fig. 7 Disadvantage of the Al-bridge structure passed over the TE generators. (a) Schematic illustration of the heat flow from the heat guide impeded at the bridge. (b) Planar temperature distribution in SOI layer in C-H-H-C device (L_{NW} = 250nm, W_{brdg} = 1.8 µm)

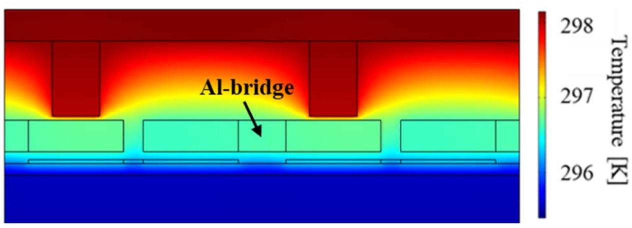

Fig. 8 Cross-sectional temperature distribution in H-C-H-C device (W_{brdg}= 37.2 µm)

Figure 8 shows the cross-sectional temperature distribution in H-C-H-C type when the W_{brdg} = 37.2 µm. The temperature profile along the Si-NW surface is shown in Fig. 6. The 37.2 µm-wide W_{brdg} has low electrical resistance, but also low thermal resistance. Thus, the temperature difference in the TE generator is diminished due to the large heat leakage through the Al-bridge from the hot side to the cold side.

The TE power of C-H-H-C and H-C-H-C type arrangements was calculated with varying the W_{brdg} from 0.1 μm to 9 μm, to find the optimum W_{brdg}. The results are shown in Fig. 9. In C-H-H-C type, the highest power is achieved when the W_{brdg} is 1.8 μm. On the other hand, in H-C-H-C type, the highest power is achieved when the W_{brdg} is 0.3 μm. The TE power of C-H-H-C type surpasses that of H-C-H-C type for all values of W_{brdg}.

Figure 10 show the TE power as a function of L_{NW} for C-H-H-C and H-C-H-C type arrangements. The TE power monotonically increases with L_{NW}. This is because the thermal resistance of Si-NW increases with L_{NW}, thereby the temperature difference across the Si-NW increases.

Figure 11 shows the areal power density vs L_{NW} for C-H-H-C and H-C-H-C type arrangements. From the view point of the areal power density, there exists optimum length L_{NW} in both types of TEGs. In both cases, the power density has a maximum at around L_{NW} = 750 nm. As, the thickness of Si substrate is reduced, the optimum NW length may shorten [6].

From these results, it is concluded that the TE power of C-H-H-C type surpasses that of H-C-H-C type arrangement even though the meander electric wiring partially hinder the injecting heat current.

IV. Conclusion

We investigated the effect of unit cell arrangements on the multi-stage-planar cavity-free unileg TE generator performance. We compared two different unit cell arrangements by FEM simulation. C-H-H-C type structure, in which the hot side of the adjacent TE generators are placed opposite to each other, exhibits higher power generation performance than H-C-H-C type. The result indicates that it is quite effective to increase the spatial interval of heat injection pitch to increase the temperature difference across Si-NW legs.

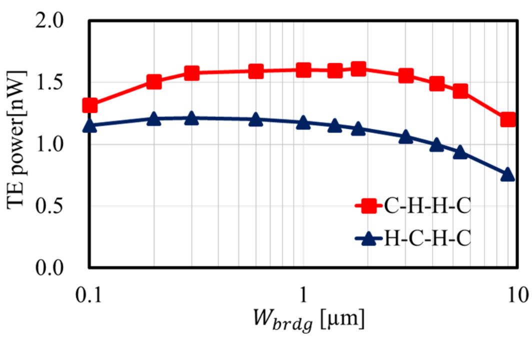

Fig. 9 TE power of H-C-H-C device and C-H-H-C device when the W_{brdg} was varied from 0.1 μm to 9 μm.

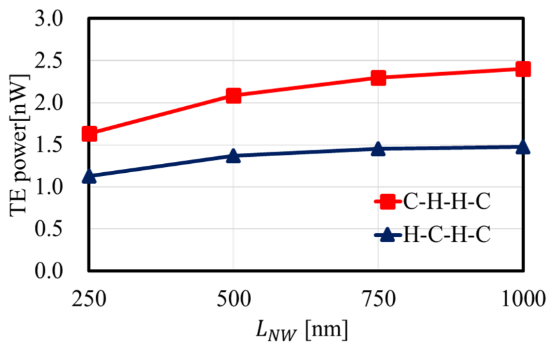

Fig. 10 TE power of H-C-H-C and C-H-H-C type devices.

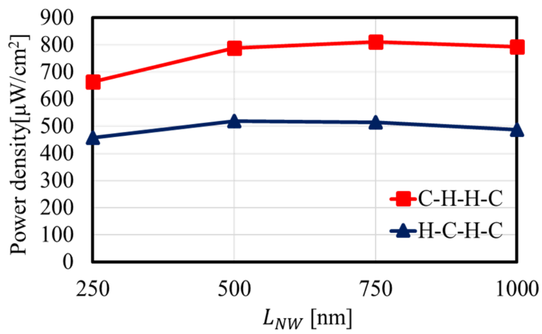

Fig. 11 Power density of H-C-H-C and C-H-H-C type devices.

V. Acknowledgment

This research is supported by JST-CREST (JPLJCR19Q5).

VI. References

[1] A. Boukai, Y. Bunimovichet, et al., "Silicon nanowires as efficient thermoelectric materials", Nature, 451.7175 (2008) 168.

[2] H. Zhang, T. Xu, S. Hashimoto, and T. Watanabe, "The Possibility of mW/cm2-Class On-Chip Power Generation Using Ultrasmall Si Nanowire-Based Thermoelectric Generators", IEEE TED 65 (2018) 2016.

[3] M. Tomita, H. Takezawa, et al., "Evaluation of Multi-stage, Unileg, Si-nanowire Thermoelectric Generator with A Cavity-free Planar Device Architecture", Ext. Abstr. SSDM (2019).

[4] Gao Min, "Chapter 11: Thermoelectric Module Design Theories", Thermoelectrics Handbook, ed. By D. M. Rowe, CRC Press, (2006).

[5] K. Oda, K. Shima, M. Tomita, T. Matsuki, and, T. Watanabe, "Optimum Design of Multi-stage Planar Unileg Thermoelectric Generator Using Si Nanowire", Abstr. JSAP Spring, (2019).

[6] K. Shima et al., "Optimum substrate design of planar type Si nanowire thermoelectric generator", Ext. Abstr. SSDM, (2018).

[7] K. Oda, M. Tomita, T. Matsukawa, T. Matsuki, and, T. Watanabe, "Backend Engineering of Cavity-free Planar Si-nanowire Thermoelectric Generator", Ext. Abstr. SSDM, (2019).

[8] T. Huesgen ,N. Kockmann, and P. Woias, "DESIGN AND FABRICATION OF A MEMS THERMOELECTRIC GENERATOR FOR ENERGY HARVESTING", Sensors and Actuators A: Physical, vol.145-146, July-August, pp.423-429 (2008).